

CFD APPLICATION TO THE REGULATORY ASSESSMENT OF FAC-CAUSED CANDU FEEDER PIPE WALL THINNING ISSUE

DONG GU KANG* and JONG CHULL JO

Korea Institute of Nuclear Safety

19 Gusong-dong, Yuseong-gu, Daejeon, 305-338, Republic of Korea

*Corresponding author. E-mail : littlewing@kins.re.kr

Received July 12, 2007

Accepted for Publication September 21, 2007

Flow fields inside feeder pipes have been simulated numerically using a CFD (computational fluid dynamics) code to calculate the shear stress distribution, which is the most important factor in predicting the local regions of feeder pipes highly susceptible to FAC (flow-accelerated corrosion)-induced wall thinning. The CFD approach, with schemes used in this study, to simulate the flow situations inside the CANDU feeder pipes has been verified as it showed a good agreement between the investigation results for the failed feedwater pipe at Surry unit 2 plant in the U.S. and the CFD calculation. Sensitivity studies of the three geometrical parameters, such as angle of the first and second bends, length of the first span between the grayloc hub and the first bend, and length of the second span between the first and the second bends have been performed. CFD analysis reveals that the local regions of feeder pipes of Wolsung unit 1 in Korea, on which wall thickness measurements have been performed so far, are not coincident with the worst regions predicted by the present CFD analysis located in the connection region of straight and bend pipe near the inlet part of the bend intrados. Finally, based on the results of the present CFD analysis, a guide to the selection of the weakest local positions where the measurement of wall thickness should be performed with higher priority has been provided.

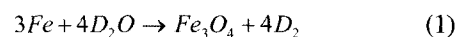
KEYWORDS : Flow-Accelerated Corrosion, CANDU Feeder Pipe, Computational Fluid Dynamics

1. INTRODUCTION

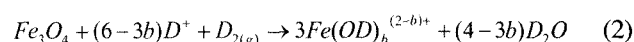
Feeder piping is an integral part of the CANDU Primary Heat Transporting System (PHTS), carrying pressurized heavy water to and from the reactor fuel channels to remove heat produced by the fission of uranium fuel [1]. The geometry and dimensions of a typical feeder pipe connected to the pressure tube are represented in Fig. 1. Heavy water passes through the annular space between the pressure tube wall and the liner and then flows into the feeder pipe through the grayloc hub vertically connected to the pressure tube.

From the results of the In-Service Inspection (ISI) measuring the wall thickness of outlet (hot-leg side) lower feeder pipes performed at two Canadian nuclear power plants, Point Lepreau and Gentilly-2 in 1995 and 1996, respectively, the wall thinning degradation of feeder pipes at the bend part was unexpectedly found to be severe. It has been well known that such wall thinning of feeder pipes is caused by the flow-accelerated corrosion (FAC) which is one of the mechanical-chemical degradation mechanisms affecting the integrity of piping systems [2].

The FAC degradation mechanism is an erosion-corrosion phenomenon due to rapid dissolution of soluble oxide film on the wall surface of carbon steel pipe or vessel subjected to turbulent water flow. For the carbon steel in heavy water, the following chemical reaction occurs, forming magnetite:



Then, some of magnetite dissolute :



The fluid flowing on the wall surface of pipe or vessel at high velocity erodes the corroded surface mechanically due to shear force on the surface by the fluid. Intensive studies to understand the parameters including shear stress, pH, etc. affecting FAC have been performed [3-6], and some commercial codes such as CHECWORKS [7] have been developed to monitor and

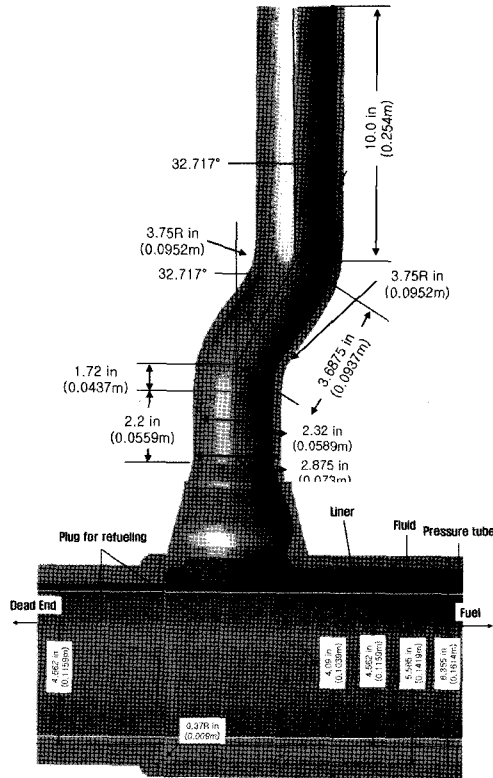


Fig. 1. Geometry and Dimensions of a Typical Feeder Pipe Connected to Pressure Tube

predict the FAC rate of piping systems/components. Corrosion depends on pH, deuterium concentration, temperature, and pipe composition, among other factors. However, erosion depends on hydrodynamic factors such as flow velocity and shear stress. Most factors, except hydrodynamic factors, uniformly affect the whole inner surface of the piping system through which the fluid flows. On the contrary, the hydrodynamic factors vary with the local position of the piping system through which the fluid flow does not maintain its velocity profile uniformly. Therefore, the high shear stress, which means the steep velocity gradient in the direction of the normal to wall surface near the pipe inner surface, will be one of the most dominant factors affecting the FAC-caused local thinning of the feeder pipe.

For Wolsung unit 1, the wall thickness measurements have been performed during every overhaul period since 1996. The wall thinning rates at the bends of outlet lower feeder pipes were assessed to exceed the design value. However, for Wolsung units 2, 3, and 4, the wall thinning rates of all the outlet lower feeder pipes were assessed not to exceed the design value. The reason is because the content of chromium in the material of feeder pipes of Wolsung units 2, 3, and 4 is higher than that of Wolsung unit 1 [4].

Up to the present, the inspection of feeder pipe wall thinning has been focused on the central extrados surface area of feeder pipe bend part, which is generally considered to be the initially most thinned area resulting from the manufacturing bending process of the feeder pipe, as shown in Fig. 2. However, the potential local areas that are expected to be the most susceptible to wall thinning due to the flow-accelerated corrosion mechanism have not been evaluated (identified). In addition, the accuracy of ultrasonic testing (UT) measurement which has been utilized is known to be unacceptably low. Thus, the present practice of feeder pipe wall thinning inspection may result in the excessive exposure of inspection personnel without achieving effective outcomes. In this regard, it will be very important to identify the local areas that are the most susceptible to the FAC-caused thinning and to determine the essential local points on which the thickness of wall needs to be measured to achieve the main objectives of inspection.

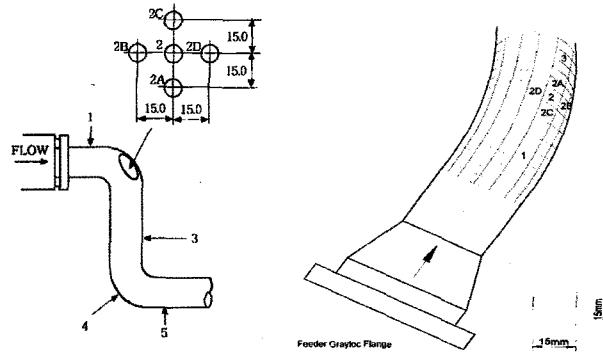


Fig. 2. Present Monitoring Points of Feeder Pipes

The flow domain including the pressure tube and the feeder pipe, which is vertically connected to the pressure tube, is very complex so that the flow velocity at the inlet of feeder pipe is not uniformly maintained. However, previous experimental and numerical studies [4, 5], which designed to predict the local area of CANDU feeder pipes susceptible to FAC-caused wall thinning, neglected the existence of pressure tube connected to the feeder pipe.

Because the geometries of the feeder pipes connected to the pressure tubes are very complex, analytic solutions to obtain the flow field are not available, and since experiments are very costly and difficult to conduct, computational fluid dynamics (CFD) analysis has been chosen as the best practical approach to address the present problem.

Therefore, in this study, the flow field inside feeder pipes has been analyzed as realistically as possible, and the shear stress distributions have been calculated to

predict the local region of the feeder pipe wall that is highly susceptible to FAC-caused thinning. Based on the results mentioned above, a guide to the selection of the weakest position (location) where the measurement of wall thickness should be performed has been provided for the establishment of preventive measures.

2. VALIDATION OF CFD APPROACH

2.1 Surry Unit 2 Wall Thinning Failure

Feedwater flowed from a 24-inch header to two 18-inch suction lines that supplied one of main feedwater pumps [8]. An elbow in the 18-inch suction line was blown out, as shown in Fig. 3 (a), and the elbow material was carbon steel. The inspection results were that the nominal wall thickness of the suction pipe was 0.5 inch. However, measurements of the wall fragment demonstrated that the wall had been generally eroded to about 0.25 inch and the thinnest areas appeared to be about 0.0625 inch. The Surry unit 2 pipe break failure mechanism was FAC [9, 10]. The detailed schematic result of Surry unit 2 wall thinning failure is described in Fig. 3 (b) [11].

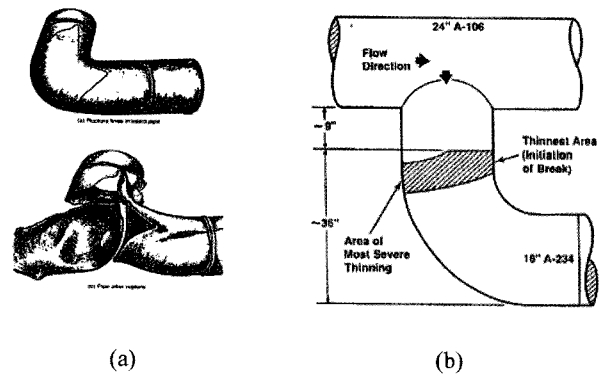


Fig. 3. Schematic Result of Surry Unit 2 Wall Thinning Failure

2.2 Problem Definition and Methodology

The piping system of Surry unit 2 at the normal operating condition is modeled to analyze the wall thinning failure by calculating shear stress distribution with CFD code, as shown in Fig. 4. The coolant is light water at a constant temperature of 188°C, and the reference pressure is equal to 3.2 MPa. The inlet condition is that the mass flow rate is equal to 1,260 kg/s, and the mass flow rate of each outlet is equal to 630 kg/s [9]. Furthermore, no slip condition is applied on the pipe wall.

CFD analysis has been performed by using CFX-5.10 code, a commercial CFD code based on a conservative finite-element based control volume method. The solution domain is divided into tetra-prism control volume cells, and about 990,000 nodes are used. The convection terms are approximated by a higher-order bounded scheme. The simulation type is steady state and the turbulent flow is simulated numerically using the shear stress transport (SST) model [12]. And a convergence criterion is that RMS residuals of major parameters are less than 0.001.

2.3 Results and Discussion

Figure 5 shows velocity vectors on a $z=0$ plane that cut across the middle of the system. The maximum velocity region is the intrados of elbow because of the momentum of the main flow and the curvature effect of the elbow bend. On the other hand, velocity near the extrados of the elbow is low at the inlet of the bend and then increases somewhat during the course of passing through the bend part. Figure 6 shows wall shear

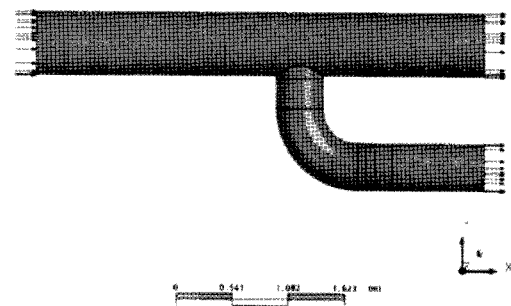


Fig. 4. System Modeling of Surry Unit 2 Wall Thinning Failure

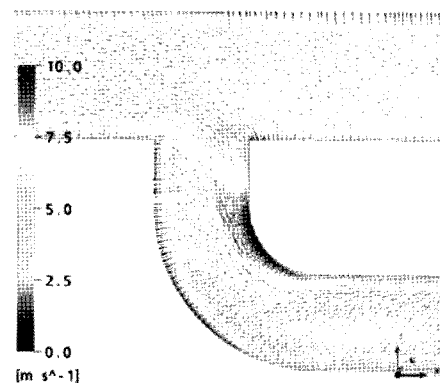


Fig. 5. Velocity Vectors for Surry Unit 2 Wall Thinning Failure (on $z=0$ Plane)

distribution on the inner surface area for Surry unit 2 wall thinning failure. The connection region between the 24-inch header and 18-inch suction line and the intrados of the elbow bend are subjected to higher wall shear. Locally highest wall shear exerts on the intrados pipe surface at the inlet part of bend.

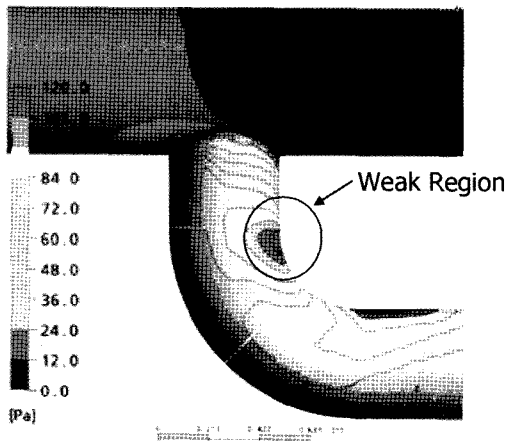


Fig. 6. Wall Shear Distribution on the Inner Surface Area for Surry Unit 2 Wall Thinning Failure

The investigation results of the failed pipe at the Surry unit 2, as shown in Fig. 3 (b), and present CFD calculation results, as shown in Fig. 6, have been compared. For a real accident, the break initiates in the intrados of the bend, which is the thinnest area, and it accords with weak region expected by CFD analysis. Thus, the CFD schemes with the CFX-5.10 code [12] used to simulate the flow situation in the CANDU feeder pipes in this study have been verified.

3. EVALUATION OF TURBULENCE MODELS

Usually, two turbulence models are used in CFD analysis. One is the shear stress transport model, and the other is the $k-\epsilon$ standard model. The SST model is conformable to the analysis of flow separation and swirl

flow and has high accuracy. However, very fine mesh is necessary, requiring a long calculation time. The $k-\epsilon$ model is conformable to the analysis of general pipe flow and gives accurate results with relatively less fine mesh in comparison with the SST model. Therefore, the $k-\epsilon$ model for the Surry unit 2 accident is used to reduce the computation time, and calculation results using the $k-\epsilon$ model are compared with those using the SST model. The total numbers of nodes used in the calculation with SST and $k-\epsilon$ model are about 990,000 and 660,000, respectively.

A comparison of both calculations using the SST and $k-\epsilon$ models is demonstrated in Figs. 7 and 8. Figure 7 shows velocity vectors for the SST model and $k-\epsilon$ model. The intrados of the elbow region has high velocity in both the SST and $k-\epsilon$ models. The wall shear distribution for the SST and $k-\epsilon$ models is compared in Fig. 8. Both the SST model and $k-\epsilon$ model predict the weak region identically, and the distribution of the velocity and wall shear calculated using the two different turbulence models are qualitatively identical and quantitatively similar. Furthermore, the difference of magnitudes of maximum shear stress on the elbow region calculated with the SST model and $k-\epsilon$ model is less than 2.4%. Therefore, through the present calculations, the effects of the turbulent models and the node numbers on the predicted local region highly susceptible to FAC-caused wall thinning were found to be negligible. Therefore, the $k-\epsilon$ standard model can be used for the simplicity and efficiency in calculations.

4. CFD ANALYSIS

4.1 Feature of Feeder Pipe

It is known that both first and second bends of outlet lower feeder pipes are the parts vulnerable to the FAC-caused wall thinning. The outlet lower feeder pipes are

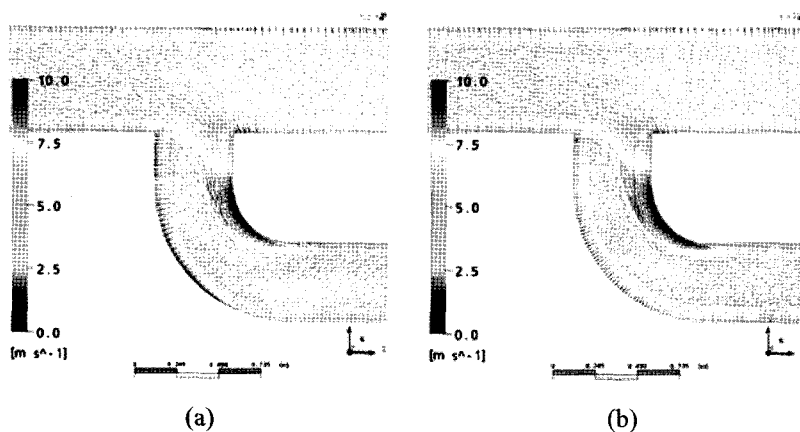


Fig. 7. Comparison of Velocity Vectors for the SST and $k-\epsilon$ Models on a $z=0$ Plane: (a) SST Model (b) $k-\epsilon$ Model

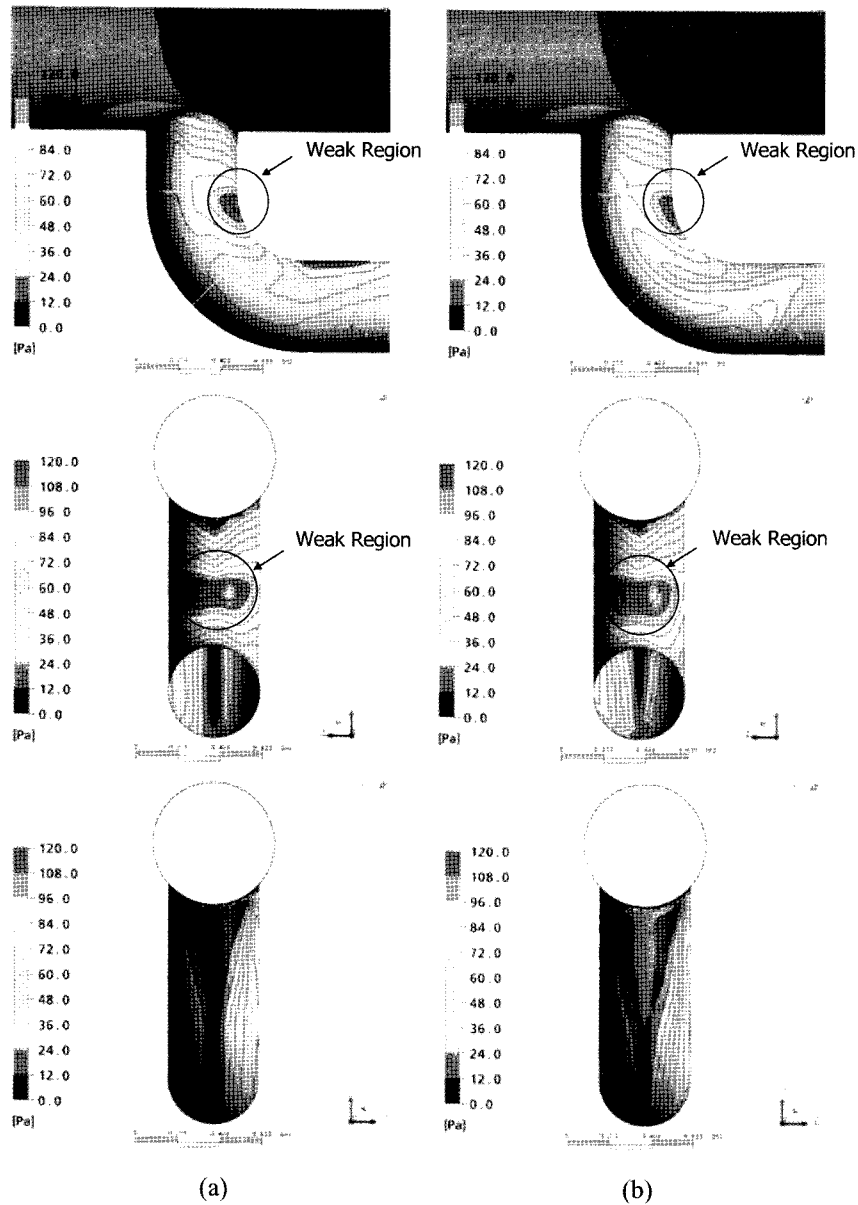


Fig. 8. Comparison of Wall Shear Distribution for the SST and $k-\epsilon$ Models: (a) SST Model (b) $k-\epsilon$ Model

classified into 20 types according to length and bend angle of the feeder pipes [4]. The 20 types of feeder pipes are grouped into two categories by the direction of the first bend outlet, as shown in Fig. 9. The first category is the geometry where the first bend winds in the upstream direction of the pressure tube. The second category is the geometry where the first bend winds in the downstream direction of the pressure tube. CFD analysis for geometric parameters is performed to investigate the effect of the first and second bend angles and the length of the straight pipe for each case. Major

parameters are indicated in Table 1, and the lengths of the first and second straight pipe which are used in this CFD analysis are referred to real data of feeder pipes.

4.2 Problem Definition and Methodology

The coolant is heavy water in a compressed liquid phase. The reference pressure is equal to 10 MPa, and the reference temperature is equal to 310°C. In terms of the inlet condition, the mass flow rate is equal to 24 kg/s, and, for the outlet condition, the average relative static pressure is equal to 0 Pa. No slip condition is applied on

Table 1. Major Parameters of CFD Analysis

First & second bend angle [deg]	Length of the first straight pipe [in]	Length of the second straight pipe [in]
30	0.6	0.98
50	0.65	1.5
70	1.89	5.76

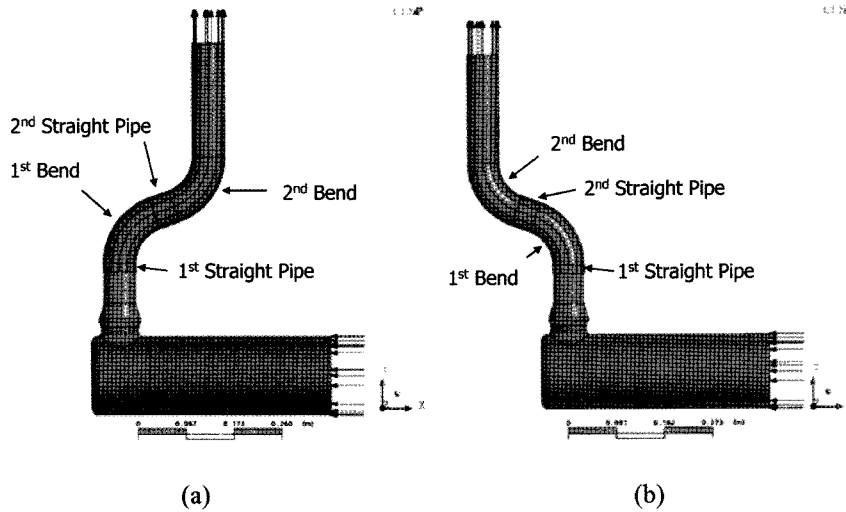


Fig. 9. Two Categories by the Direction of the First Bend Outlet: (a) First Bend Winds in the Upstream Direction of the Pressure Tube, (b) First Bend Winds in the Downstream Direction of the Pressure Tube

the wall. These conditions are referred to FSAR [1].

CFD analysis has been performed by using CFX-5.10 code. The solution domain is divided into tetra-prism control volume cells, and about 900,000 nodes are used. The convection terms are approximated by a higher-order bounded scheme. The simulation type is steady state, and the turbulent flow is simulated numerically using the standard *k-ε* turbulence model [12]. Furthermore, a convergence criterion is that RMS residuals of major parameters are less than 10^{-6} .

4.3 Type A Feeder Pipe: The Case Where the First Bend Winds in the Upstream Direction of the Pressure Tube [See Fig. 9 (a)]

• Effects of the bend angle

To investigate the effects of pipe bend angle on the shear stress distribution on the inner wall, the calculations have been performed for the three feeder pipes having different a first bend angle (which is the same as the second bend angle) of 30, 50, or 70 degrees while the lengths of the first and second straight pipes are fixed at

0.65 and 1.5 inches, respectively. Figure 10 shows the pressure drop and the magnitude of maximum wall shear according to the variation of the bend angle. A pressure drop increases linearly as the bend angle increases, and the magnitude of the maximum wall shear increases as the bend angle increases. The location of the maximum wall shear, which is a weak region due to FAC, is demonstrated in Fig. 11. The cross symbol indicates the location of the maximum wall shear. The weakest region subjected to the maximum wall shear is located at the second bend intrados surface region between the inlet part of the second bend and the mid part of the second bend for all cases.

• Effects of the second straight pipe length

The three different second straight pipe lengths of 0.98, 1.5, and 5.76 inches with the same first and second bend angles of 70 degrees and the first straight pipe length of 0.65 inch have been considered in the calculations to investigate the effects of the second straight pipe length on the shear stress distribution on the inner wall. Figure 12 shows the pressure drop and the magnitude of the

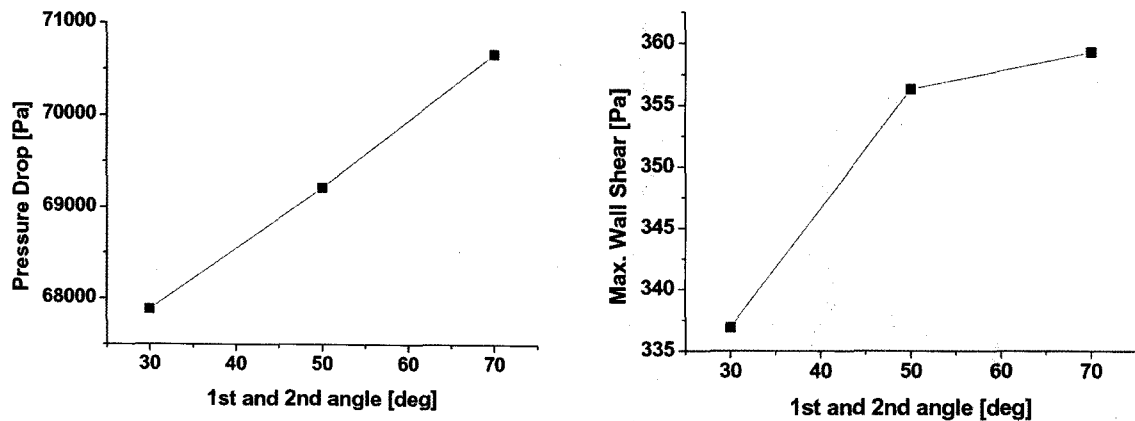


Fig. 10. Effects of the Bend Angle of Type A Feeder Pipe on the Pressure Drop and Maximum Wall Shear

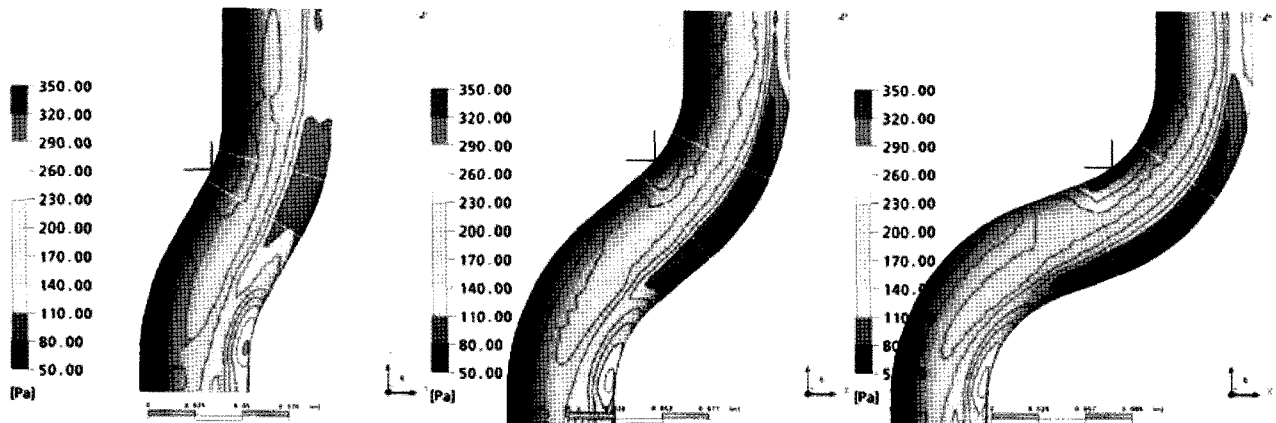


Fig. 11. Effects of the Bend Angle of Type A Feeder Pipe on the Location Subjected to the Maximum Wall Shear

maximum wall shear according to the variation of the length of the second straight pipe. The pressure drop increases as the length of the second straight pipe increases, and the magnitude of the maximum wall shear decreases because flow is developed as the length of the second straight pipe increases. The location of the maximum wall shear, which is the weak region due to FAC, is demonstrated in Fig. 13. The weakest region subjected to the maximum wall shear is located at the second bend intrados surface area for all cases and between the inlet part of the second bend and mid part of the second bend, like in previous cases. The location of maximum wall shear leans more to the inlet part of the second bend as length of the second straight pipe increases.

• Effects of the first straight pipe length

The three different first straight pipe lengths of 0.6, 0.65, and 1.89 inches with the same first and second bend angles of 70 degrees and the second straight pipe length of 0.98 inch have been considered in the calculations. Figure 14 shows the pressure drop and the magnitude of maximum wall shear according to the variation of the length of the first straight pipe. The pressure drop increases as length of the first straight pipe increases, and magnitude of the maximum wall shear decreases because flow is developed as the length of the first straight pipe increases. The weakest region subjected to the maximum wall shear is located at the second bend intrados surface area for all cases and between the inlet part of the second

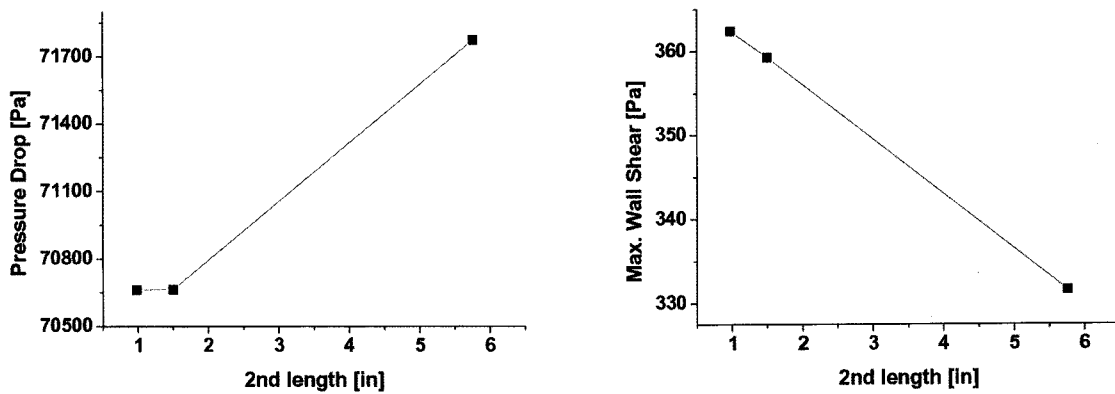


Fig. 12. Effects of the Second Straight Span Length of Type A Feeder Pipe on the Pressure Drop and Maximum Wall Shear

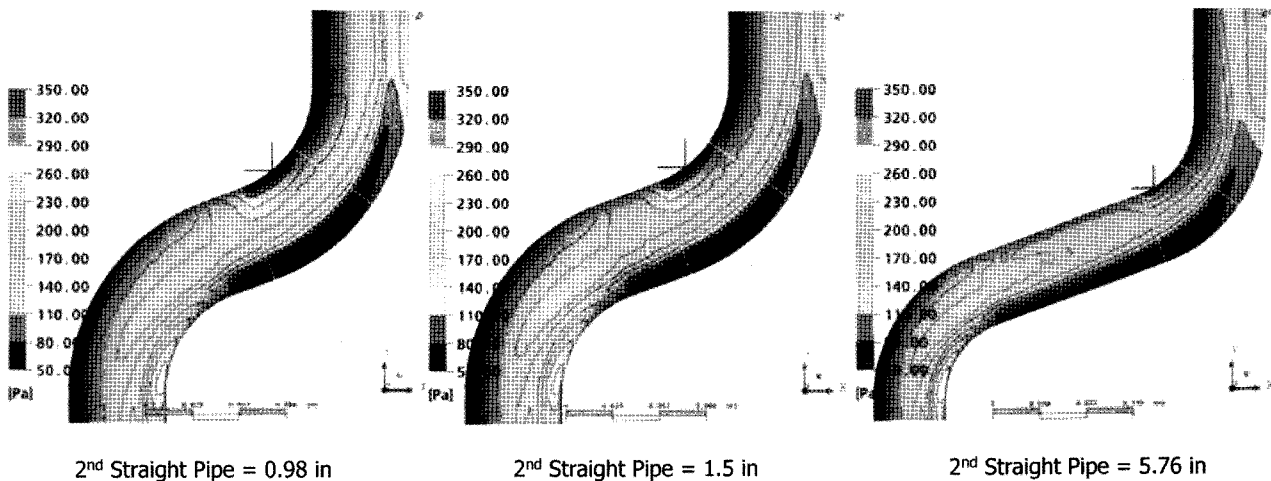


Fig. 13. Effects of the Second Straight Span Length of Type A Feeder Pipe on the Location Subjected to the Maximum Wall Shear

bend and mid part of the second bend, like in previous cases, as demonstrated in Fig. 15.

4.4 Type B Feeder Pipe: The Case Where the First Bend Winds in the Downstream Direction of the Pressure Tube (See Fig. 9 (b))

• Effects of the bend angle

The same specified values of the parameters as applied for the previous investigations of the effect of the bend angle for type A feeder pipe are applied. The pressure drop and the magnitude of the maximum wall shear increase as the bend angle increases, as shown in Fig. 16. The location of the maximum wall shear, which is the weak region due to FAC, is demonstrated in Fig.

17. The weakest region subjected to the maximum wall shear is located at the first bend intrados surface area and between the inlet part of the first bend and mid part of the first bend for all cases.

• Effects of the first straight pipe length

To investigate the effects of the first straight pipe length on the shear stress distribution on the inner wall, the calculations have been performed for the three feeder pipes having different first straight pipe lengths of 0.6, 0.65, or 1.89 inches while the first and second bend angles and the length of the second straight pipe are fixed to 70 degrees and 1.5 inches, respectively. Figure 18 shows the pressure drop and the magnitude of the maximum wall shear according to the variation of the

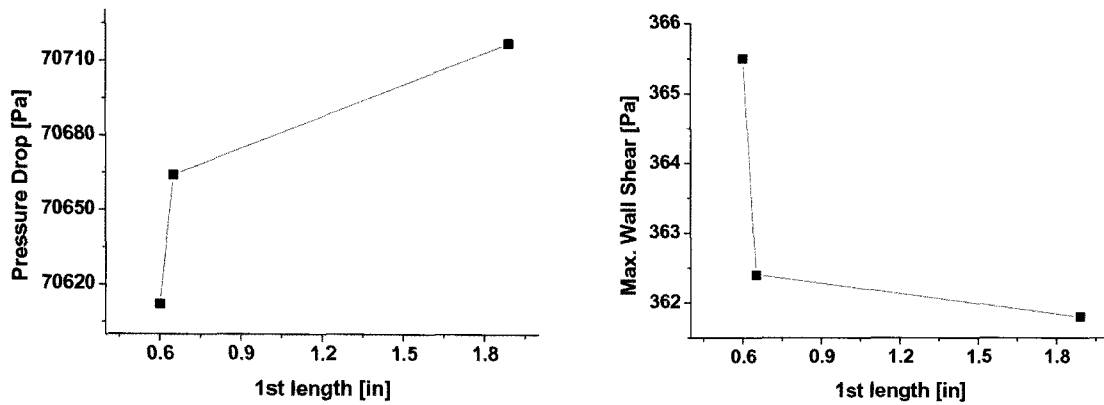


Fig. 14. Effects of the First Straight Span Length of Type A Feeder Pipe on the Pressure Drop and Maximum Wall Shear

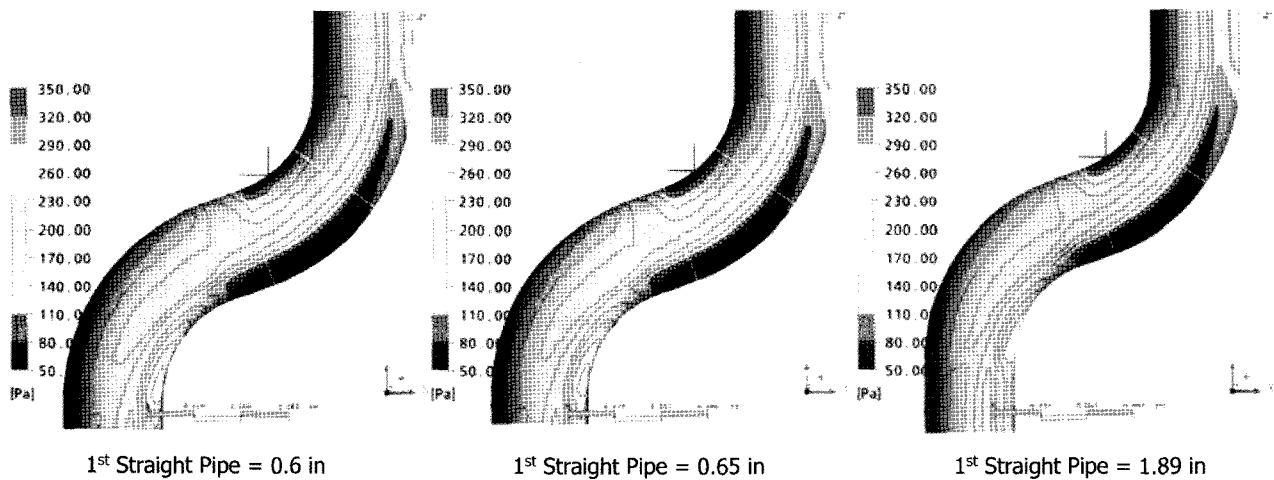


Fig. 15. Effects of the First Straight Span Length of Type A Feeder Pipe on the Location Subjected to the Maximum Wall Shear

length of the first straight pipe. In this case, the pressure drop decreases as the length of the first straight pipe increases because the friction due to turbulence, which is proportional to the pressure drop, increases as the length of the first straight pipe decreases. The magnitude of the maximum wall shear decreases because the flow is developed as the length of the first straight pipe increases. The weakest region subjected to the maximum wall shear is located at the first bend intrados surface area between the inlet part of the first bend and mid part of the first bend like previous cases, as demonstrated in Fig. 19.

• Effects of the second straight pipe length

Based on the fact that the weakest region subjected to the maximum wall shear is located at the first bend

intrados surface region between the inlet part of the first bend and mid part of the first bend for all cases, the effects of the second straight pipe length on the fluid shear stress distribution are expected to be negligible.

4.5 Results and Discussion

As shown in Fig. 20, in the case where the first bend winds in the upstream direction of the pressure tube, the location subjected to the maximum wall shear stress is located at the intrados surface between the inlet part of the second bend and mid part of the second bend. Because the location of the maximum wall shear stress leans toward the inlet part of second bend, the connection region of the straight and bend pipe near the inlet part of the second bend intrados is predicted to be the region most

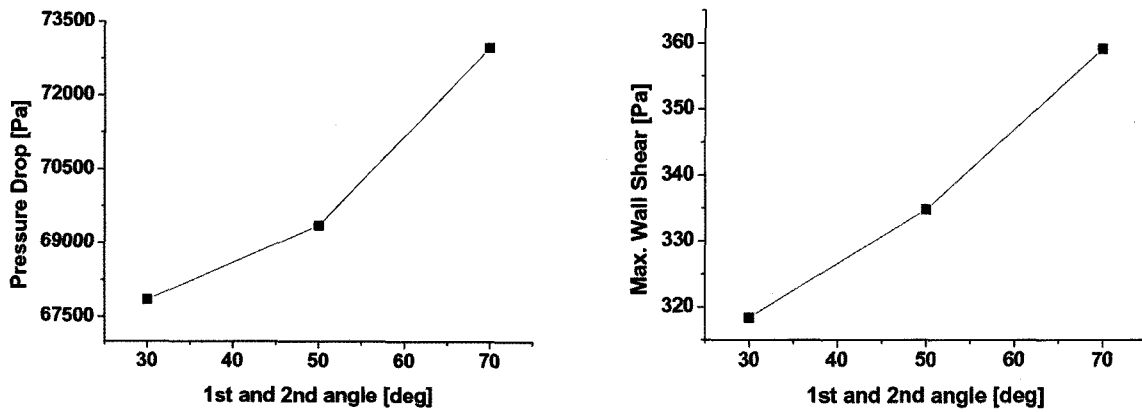


Fig. 16. Effects of the Bend Angle of Type B Feeder Pipe on the Pressure Drop and Maximum Wall Shear

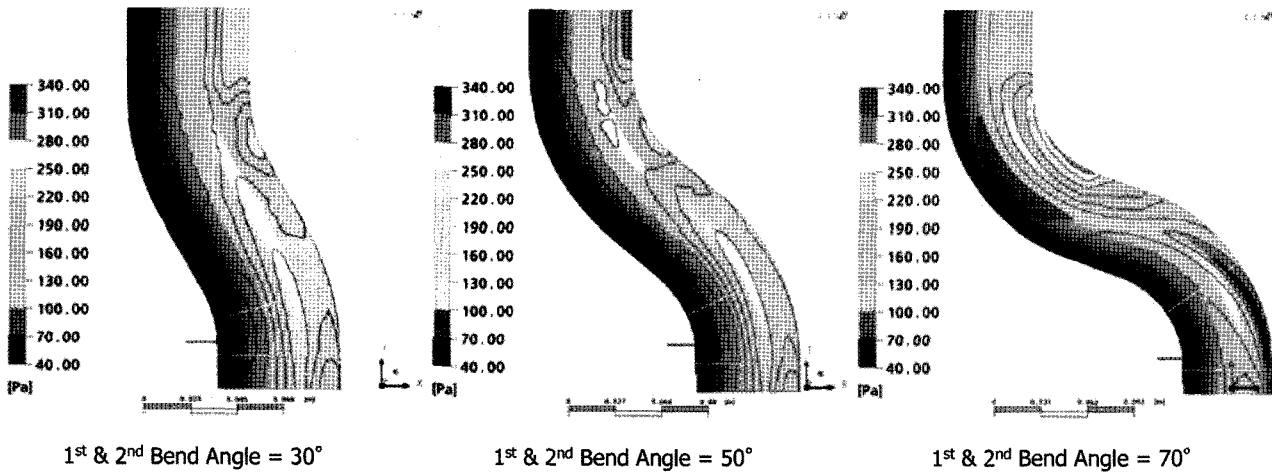


Fig. 17. Effects of the Bend Angle of Type B Feeder Pipe on the Location Subjected to the Maximum Wall Shear

susceptible to wall thinning due to FAC. Furthermore, it is possible that region of the second straight pipe, where the second bend begins, may be weaker than the intrados area of bend that is thickened by the bending process.

As shown in Fig. 21, in the case where the first bend winds in the downstream direction of the pressure tube, the connection region of straight and bend pipe near the inlet part of the first bend intrados is predicted to be the worst region because the maximum wall shear leans toward the inlet part of first bend. Furthermore, the region of first straight pipe where the first bend begins may be weaker than the intrados area of bend that is thickened by bending process.

By comparing present monitoring points with the result of CFD analysis, the present wall thickness measurement points (wall integrity monitoring points) of

the feeder pipe are shown to be not coincidental with the worst region predicted by the CFD analysis. In site, feeder pipe monitoring points are concentrated in a central region on bend extrados, which is the thinnest area because of the bending process. However, in this study, the connection region of straight and bend pipes near the inlet part of the bend intrados is predicted to be the region most susceptible to wall thinning due to FAC. Furthermore, it was confirmed during a technical meeting with AECL staff that FAC rates on bend intrados were more significant than bend extrados [13]. Considering all these factors, a regulatory position has been made to include wall thickness measurement on first and second bend intrados of outlet lower feeder pipes in the current inspection system since the 19th Wolsung unit 1 ISI performed in November, 2006.

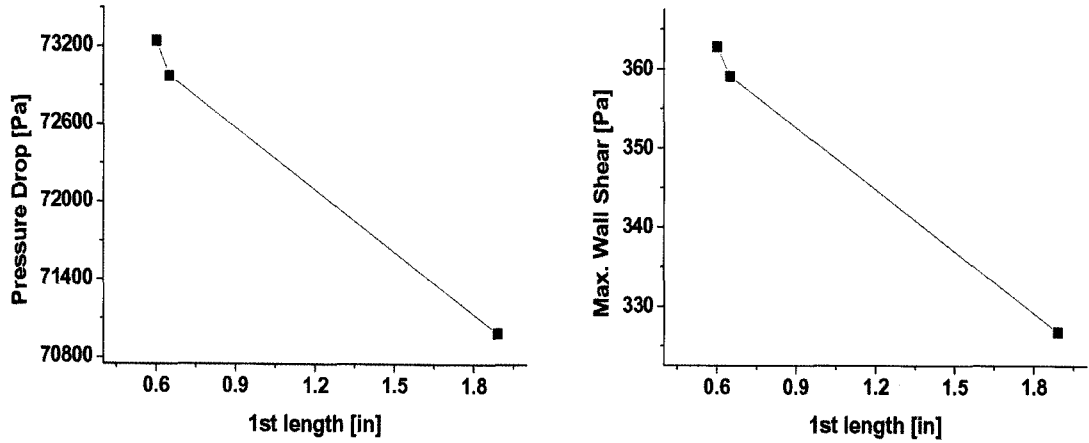


Fig. 18. Effects of the First Straight Span Length of Type B Feeder Pipe on the Pressure Drop and Maximum Wall Shear

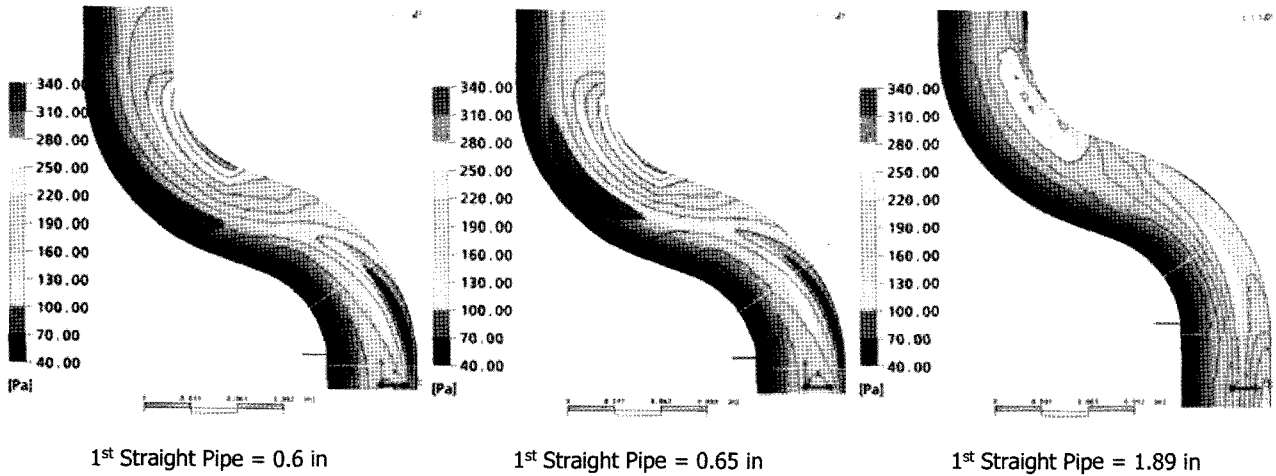


Fig. 19. Effects of the First Straight Span Length of Type B Feeder Pipe on the Location Subjected to the Maximum Wall Shear

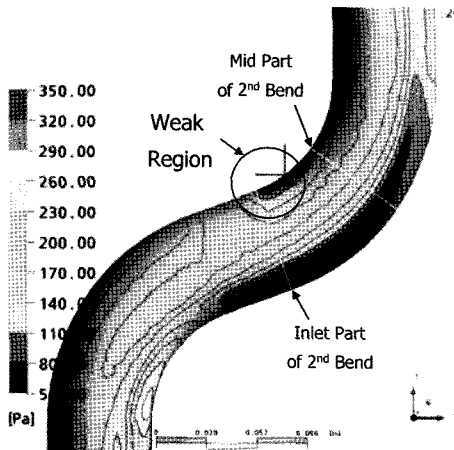


Fig. 20. Weak Region Due to FAC in the Case Where the First Bend Winds in the Upstream Direction of the Pressure Tube

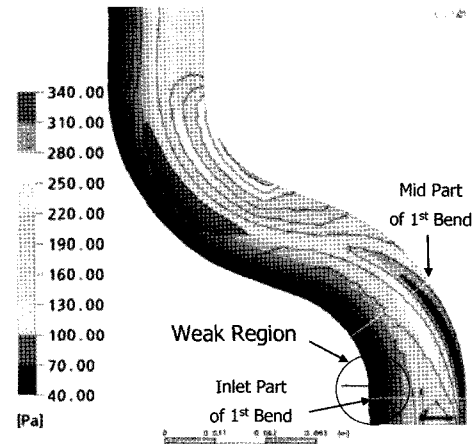


Fig. 21. Weak Region Due to FAC in the Case Where the First Bend Winds in the Downstream Direction of the Pressure Tube

5. CONCLUSIONS

Flow fields inside feeder pipes have been simulated numerically using a CFD code to predict the local regions of the feeder pipes highly susceptible to FAC-induced wall thinning. The CFD approach with schemes used in this study to simulate the flow situations inside the CANDU feeder pipes has been verified by showing a good agreement between the investigation results for the failed feedwater pipe at the Surry unit 2 plant in U.S. and the CFD calculation. The local regions of feeder pipes of the Wolsung units in Korea, on which the wall thickness measurements have been performed so far, were found to be not coincidental with the worst regions predicted by the present CFD analysis, which are the connection region of the straight and bend pipe near the inlet part of the bend intrados. Based on the results of this CFD analysis, a guide to the selection of the weakest local positions where the measurement of wall thickness should be performed with higher priority has been provided.

REFERENCES

- [1] KHNP, "Wolsung Unit 1 Final Safety Analysis Report," Korea Hydro & Nuclear Power.
- [2] AECL, "Feeder Wall Thickness Measurements," CANDU-6 Station Information Bulletin 96-2, Atomic Energy of Canada Limited, 1996.
- [3] B. Chexal, et al., "Flow-Accelerated Corrosion in Power Plants," EPRI-TR-106611-R1, Electric Power Research Institute (1998).
- [4] KHNP, "Development of Technologies to Monitor for Feeder Thinning of CANDU Nuclear Power Plants," Final Research Report, Korea Hydro & Nuclear Power (2002).
- [5] KEPRI, "Development of Prediction and Control Technology for Aging of Feeder Piping," Final Research Report, Korea Electric Power Research Institute (2005).
- [6] Jo, J.C., Kim, Y.I., Shin, W.K., and Choi, S.K., "Numerical Analysis of Three-dimensional Turbulent Flow in Curved Pipes," 1999 KNS Autumn Meeting, Seoul, Korea, 1999
- [7] EPRI, "CHECWORKS™ Computer Program Users Guide," EPRI-TR-103198-P1, Electric Power Research Institute (1997).
- [8] Vikram N. Shah, and Philip E. MacDonald, *Aging and Life Extension of Major Light Water Reactor Components*, p.522, Elsevier, Amsterdam, The Netherlands (1993).
- [9] USNRC, "Feedwater Line Break," Information Notice 86-106, United States Nuclear Regulatory Commission (1986).
- [10] USNRC, "Feedwater Line Break," Information Notice 86-106, Supplement 1, United States Nuclear Regulatory Commission (1987).
- [11] Kim, J.W., "Recent Research Status for Wall Thinning Integrity Assessment of Piping System in Nuclear Power Plants," *New Technology Workshop for the Remote Maintenance/Surveillance in Nuclear Power Plant: 2006 KNS Spring Meeting*, Chuncheon, Korea, May 25-26, 2006.
- [12] ANSYS, "CFX-5.10 Manual," ANSYS, Inc (2005)
- [13] John Pietralik, "Modeling of FAC in Feeders," *Technical Meeting between KINS and COG/AECL, AECL*, Toronto, Oct. 16, 2006.